

# Multifrequency Coupled-Resonator Sensor for Dielectric Characterization of Liquids

Lyda Vanessa Herrera Sepulveda<sup>1</sup>, Jose Luis Olvera Cervantes<sup>2</sup>, and Carlos E. Saavedra<sup>1</sup>

**Abstract**—A six-band microstrip sensor, based on a pair of electrically coupled resonators (ECRs), is proposed to perform multifrequency dielectric characterization of liquids. A pocket is milled through the substrate bottom of the sensor to contain the fluid sample, avoiding the need for a sample holder. The pocket has been designed to achieve a higher electric field magnitude in the sensing region and a mechanism to separate the resonant frequencies, which helps to ensure a high span between the first and the last resonant frequency. The microstrip sensor is implemented on a 1.905-mm-thick substrate with  $\epsilon'_r = 12.2$  and  $\tan \delta = 0.0019$ . The sensor's six resonance frequencies span the range between 1 and 3.5 GHz. Experimental tests show that the sensor can measure a wide range of  $\epsilon'_r$  values between 2 and 79 resulting in close similarities to the dielectric constants published in previous works.

**Index Terms**—Coupled resonators, dielectric constant, liquid characterization, microwave sensor, multiband sensor, relative permittivity.

## I. INTRODUCTION

PERMITTIVITY characterization of liquids is a subject of wide research interest at radio frequency (RF) and the microwave frequency range [1]–[7]. RF and microwave liquid sensors for determining the real part of the relative permittivity, or dielectric constant ( $\epsilon'_r$ ), have been widely proposed for different applications, such as quality control on industrial liquids [8]–[10], detection or adulteration in liquids [11], and medical applications [12], [13].

Some well-known advantages of microstrip-based sensors are low cost, easy fabrication, and real-time operation [1], [2], [14], [15]. Different microstrip resonators have been presented in the literature to determine the liquid's permittivity [3], [5]–[8], [11], [14]–[19]. For example, in [6], [8], [11], and [18], complementary split-ring resonators (CSRRs) are used; in [3], a symmetric splitter-combiner configuration loaded with a pair of identical SRRs is presented; or a

modified SRR configuration based on multiple SRRs [14] have also been used. Other sensors using an open-loop resonator (OLR) [17] and an OLR based on a stepped-impedance-resonator [7] have been reported. Coupled structures have also been employed as permittivity sensors for liquids, using a resonant perturbation technique or the curve fitting technique [1], [2], [15], [19].

Moreover, planar microstrip sensors have been implemented to work in multiple frequency bands. In [16], a square ring resonator was used to determine  $\epsilon'_r$  for the liquid samples over the three frequencies, 1, 2, and 3 GHz. In addition, the liquid's sample was held inside a glass capillary. In [17],  $\epsilon'_r$  liquid measurements were performed at three resonant frequencies using three different OLRs and their corresponding dielectric liquid holders. Another multiresonator sensor working at 2.5, 3.5, and 4.5 GHz is presented in [20], where a microfluidic channel was used.

In [21], a nonidentical double-SRRs (NID-SRRs) sensor was used to determine  $\epsilon'_r$  of liquids at two resonant frequencies, 5.76 GHz and 7.85 GHz, where two measurements were required to obtain the two resonance frequencies. Other dual-band sensors for liquid characterization are presented in [6] and [7], where a CSRR and a microstrip OLR symmetrically fed, respectively, have been proposed as liquid sensors operating at 2.45 and 5.80 GHz. In both cases, a microfluidic glass tube was used as a liquid sample holder.

On the other hand, electrically coupled resonators (ECR) have been used as filters [22], and in some cases as dielectric constant sensors for planar and liquid samples [23], [24]. In the case of liquid samples [23], a container is placed over the ECR sensor and the measurements are performed in a single-frequency band.

It is well known that the permittivity is a function of frequency and that significant changes are present at low frequencies [1], [25]; however, the microstrip sensors reported in the literature operate in single-, two-, or three-frequency bands using sample holders or microfluidic channels [7], [16]–[21].

In this article, a six-band microstrip sensor for liquid characterization is proposed. The microstrip sensor is based on a pair of OLRs fed by T-shaped input–output (I/O) networks, and the dielectric of the substrate is modified to have a pocket, where the ground (GND) plane is restored with a segment of adhesive-backed copper foil. When two OLR are coupled two resonant frequencies, electric ( $f_e$ ) and magnetic ( $f_m$ ), occur around the fundamental resonance of the uncoupled single resonator ( $f_n$ , where  $n = 0, 1, 2, \dots$ ). In this work, it has been exploited the resonant frequencies  $f_{e0}$  and  $f_{m0}$  around

Manuscript received July 15, 2021; revised October 8, 2021; accepted October 13, 2021. Date of publication October 22, 2021; date of current version November 4, 2021. This work was supported in part by the Discovery Grant from the Natural Sciences and Engineering Research Council of Canada under Grant RGPIN/04784-2016; and in part by the Consejo Nacional de Ciencia y Tecnologia, Mexico, under Grant 487558. The Associate Editor coordinating the review process was Tae-Weon Kang. (Corresponding author: Lyda Vanessa Herrera Sepulveda.)

Lyda Vanessa Herrera Sepulveda and Carlos E. Saavedra are with the Department of Electrical and Computer Engineering, Queen's University, Kingston, ON K7L 3N6, Canada (e-mail: 19lvhs@queensu.ca; saavedra@queensu.ca).

Jose Luis Olvera Cervantes is with the Instituto Nacional de Astrofisica, Optica y Electronica, Puebla 72840, Mexico.

Digital Object Identifier 10.1109/TIM.2021.3122116

1557-9662 © 2021 IEEE. Personal use is permitted, but republication/redistribution requires IEEE permission.  
See <https://www.ieee.org/publications/rights/index.html> for more information.

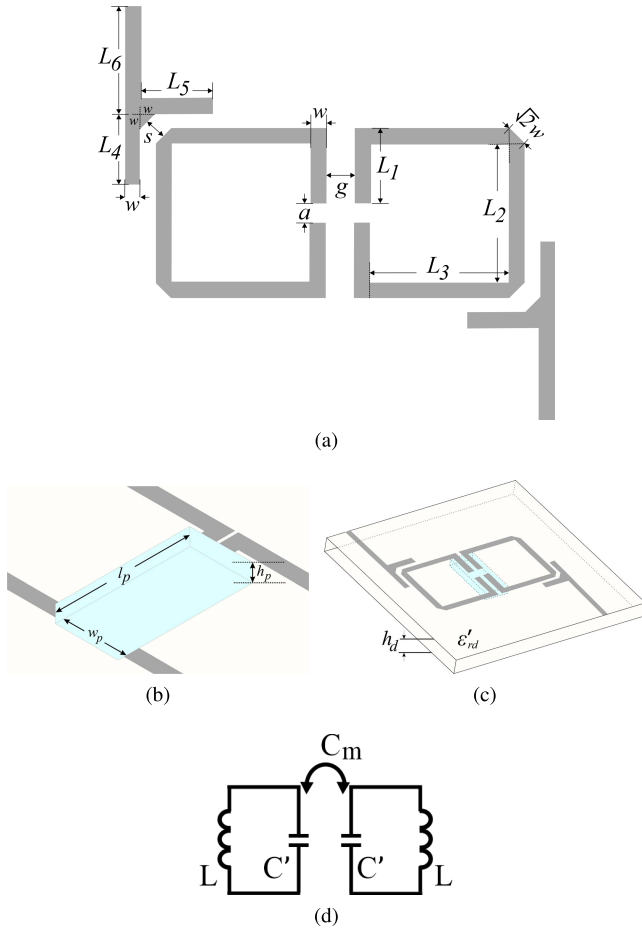


Fig. 1. Six-band ECR proposed sensor. (a) Top view dimensions. (b) Rectangular Pocket dimensions. (c) 3-D view. (d) ECR model.

$f_0$ ,  $f_{e1}$  and  $f_{m1}$  around  $f_1$ , and  $f_{e2}$  and  $f_{m2}$  around  $f_2$  to ensure the measurements at six resonant frequencies. For the dielectric constant measurements, both  $f_{en}$  and  $f_{mn}$  should be well separated; however, this is not a trivial task. Therefore, a pocket has been included as a sample holder avoiding the use of an external liquid holder, as well as a mechanism to separate  $f_{en}$  and  $f_{mn}$ , and also to ensure a high span between the first and the last resonant frequency. The loss tangent is not considered because it does not produce a significant enough change over the resonant frequencies [26]. All of the above-mentioned sensor characteristics are explained in Section II. The sensing principle and the methodology are presented in Section III, and the experimental results are shown in Section IV. Finally, Section V summarizes the main conclusions.

## II. PROPOSED SENSOR

The proposed six-band microstrip sensor for liquid dielectric constant sensing is shown in Fig. 1. The sensor is formed by a pair of ECR and T-shaped I/O networks on a TMM® thermoset microwave material laminate, TMM13i substrate [27], with a dielectric material thickness  $h_d = 1.905$  mm, dielectric constant  $\epsilon'_{rd} = 12.2$ , and a loss tangent of 0.0019, operating at 1 GHz. In Fig. 1(b) is shown that the pocket's shape and sizes which have been optimized to achieve a higher electric field magnitude in the sensing region and a mechanism to

separate the resonant frequencies (coupling coefficient), which helps to ensure a high span between the first and the last resonant frequency. The pocket sizes are 6 mm in width ( $w_p$ ), 12 mm in length ( $l_p$ ), and 1.67 mm in height ( $h_p$ ), allowing for a sample volume at 120  $\mu$ L. The TMM13i substrate is used because its electrical properties allow for a narrow microstrip transmission line (TL) at a low resonance frequency (around 1 GHz), and its mechanical properties allow for a stiff sensor where the liquid sample can be placed directly in the pocket.

### A. Microstrip Six-Band ECR Sensor

In Fig. 1(a), the six-band ECR sensor sizes are shown, and they were obtained from the basic ECR microstrip theory, as presented in [28]. All microstrip TL have 50  $\Omega$  as the characteristic impedance. The resonators are separated from each other by a gap distance of  $g = 0.3$  mm. The width of each resonator is  $w = 1.38$  mm, and the total length is  $L_T = 52$  mm, where  $L_1 = 6.68$  mm and  $L_2 = L_3 = 12.42$  mm. The resonators are arranged as open loops with endings separated by the distance  $a = 1.8$  mm. Two-square ECR's bends are modified to minimize the reactance due to the discontinuity between the ECR and the I/O coupling TL. The chamfered bend's value can be expressed as  $(2)^{1/2} w$  in two of the four ECR bends, as shown in Fig. 1(a). They were chamfered using one of the discontinuity techniques presented in [29].

The I/O networks are two T-shaped microstrip TLs placed at each side of the square ECR and at the opposite side of the ECR, as shown in 1(a). The opposite side is selected such that the phase response indicates electrically coupled resonance ( $S_{21}$  phase = 180°), as a result, the sensor is out-of-phase and can be called an ECR sensor. Other configurations cannot be selected because it is a magnetically coupled case ( $S_{21}$  phase = 0°). The I/O network lengths are  $L_4 = L_5 = 6.4$  mm, and  $L_6 = 14.1$  mm corresponding to a quarter-wavelength, and the width is  $w = 1.38$  mm. Additionally, a TL with one chamfered edge is used. The separation between the I/O T-shaped microstrip networks and the square ECR is given by  $s = 0.3$  mm. The position, shape, and sizes of the I/O networks are designed so that the sensor reaches multiple frequency bands in the frequency response.

### B. Sensing Pocket

As noted earlier, the dielectric of the substrate has a pocket milled out, centered below the gap  $g$  between the two resonators, that holds the liquid sample inside. Fig. 2 shows the  $S_{21}$ -parameter responses of the ECR sensor for simulation and experimental results, with an air-filled pocket and without the pocket, and their resonant frequencies are summarized in Table I. The deviations between the simulation and experimental resonant frequencies, for the ECR sensor with an air-filled pocket, are mainly due to the fabrication errors and possible variations in the permittivity value of the substrate. In Fig. 2, it can be noticed that the span between  $f_1$  and  $f_6$  is wider in the ECR sensor with the presence of the pocket response (2.374 GHz) than without it (2.073 GHz).

Considering the wider span between the first ( $f_1$ ) and the sixth ( $f_6$ ) resonant frequency from the simulations, the shape

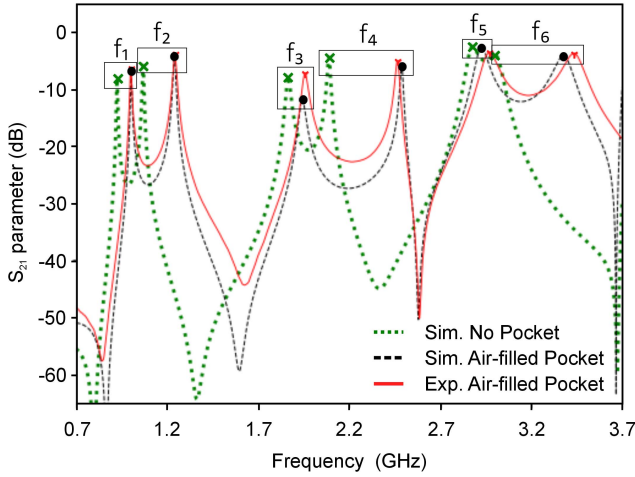


Fig. 2. Frequency response of the multifrequency ECR sensor. Comparison between the ECR simulated sensor with and without the pocket, and the ECR experimental sensor.

TABLE I  
RESONANT FREQUENCIES VALUES

Freq.		Sim. No Pocket (GHz)	Sim. Air-filled Pocket (GHz)	Exp. Air-filled Pocket (GHz)
$f_1$	$f_e$	0.926	1.001	1.001
$f_2$	$f_m$	1.068	1.244	1.244
$f_3$	$f_m$	1.866	1.943	1.957
$f_4$	$f_e$	2.089	2.489	2.467
$f_5$	$f_m$	2.878	2.928	2.970
$f_6$	$f_e$	2.999	3.377	3.436

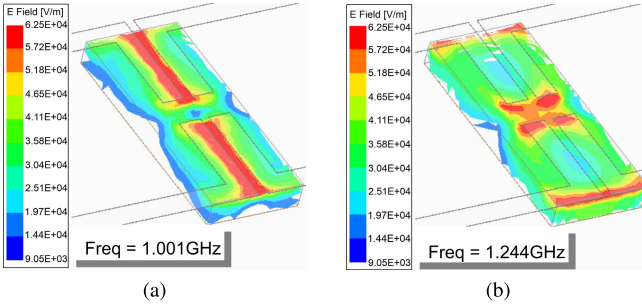


Fig. 3. Fundamental harmonic's E-field magnitude. (a) First resonance frequency due to the presence of the electric wall,  $f_1$  ( $f_e$ ). (b) Second resonance frequency due to the presence of the magnetic wall,  $f_2$  ( $f_m$ ).

and the dimensions of the pocket were chosen. As a result, the achieved electric field (E-field) magnitudes in the pocket of the sensor at the fundamental harmonic,  $f_1$  ( $f_e$ ) and  $f_2$  ( $f_m$ ), are as high as  $6.25 \times 10^4$  V/m, as shown in Fig. 3.

### III. SENSING PRINCIPLE AND METHODOLOGY

A lossless equivalent circuit for the ECR sensor with the pocket is shown in Fig. 1(c), where  $L$  is the resonator's inductance,  $C_m$  is the mutual capacitance, and  $C'$  represents the total capacitance. They are related to the electric and magnetic resonant frequencies,  $f_e$  and  $f_m$  (at the first harmonic  $f_1$  and  $f_2$ , respectively), as [22]

$$f_e = \frac{1}{2\pi\sqrt{L(C' + C_m)}} \quad (1)$$

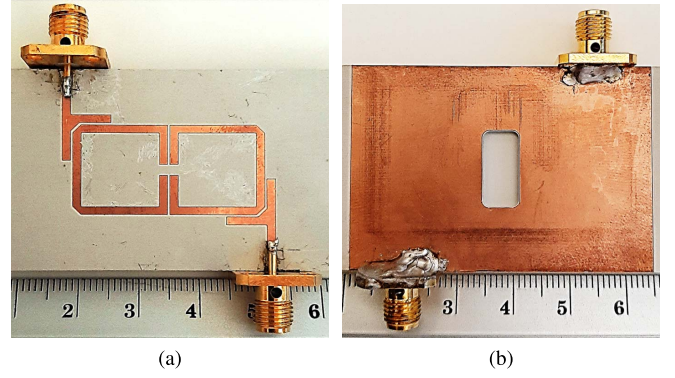


Fig. 4. Fabricated six-band ECR sensor with a pocket. (a) Top and (b) bottom views.

$$f_m = \frac{1}{2\pi\sqrt{L(C' - C_m)}}. \quad (2)$$

The total capacitance is formed by the resonator and pocket's capacitances ( $C$  and  $C_p$ , respectively), given by

$$C' = \left(\frac{1}{C} + \frac{1}{C_p}\right)^{-1}. \quad (3)$$

The liquids permittivity as a function of resonance frequency, using the curve fitting method, assumes a nonlinear relation between the independent variable and the dielectric constant [7], [30]. The relation between each resonance frequency and  $\epsilon'_r$  of a liquid can be expressed by

$$\epsilon'_r = \rho_{1n} f_n^{\rho_{2n}} + \rho_{3n} \quad (4)$$

where  $\rho_{1n}$ ,  $\rho_{2n}$ , and  $\rho_{3n}$  are fitting constants, and  $n$  represents the resonance frequency number, from 1 to 6.

In Fig. 4, the fabricated six-band ECR sensor with a pocket is shown. It is worth mentioning that the ECR sensor can be designed to work at other frequencies while using the proposed sensing principle for liquid characterization. To pattern the ECR sensor and to mill out the pocket, an LPKF ProtoMat E44 circuit plotter was used. The experimental sensing methodology consists of the following steps:

- 1) The  $S$ -parameters of the empty sensor are obtained, and the experimental  $S_{21}$ -parameter is the measurement reference.
- 2) The pocket is filled with the liquid sample, and the  $S$ -parameters are measured.
- 3) The pocket is cleaned using isopropyl alcohol as a first clean step to remove excess liquid from the pocket wall. In the second clean step, DI water was used to remove any other liquid or particle remaining.
- 4) Finally, the empty sensor is measured again, and its  $S_{21}$ -parameter is compared with the measured reference in step 1 to ensure the pocket is clean. We highlight that the pocket is open at each measurement.

In this work, the methodology in [24] is used for liquid samples. The proposed (7) is solved to find the fitting constants  $\rho_{1n}$ ,  $\rho_{2n}$ , and  $\rho_{3n}$  at each resonance frequency, using three known calibration liquids (KCL1, KCL2, and KCL3). The sensor is filled with each KCL and restored with a segment of adhesive-backed copper foil, and the experimental single-ended  $S$ -parameters are obtained. Subsequently,

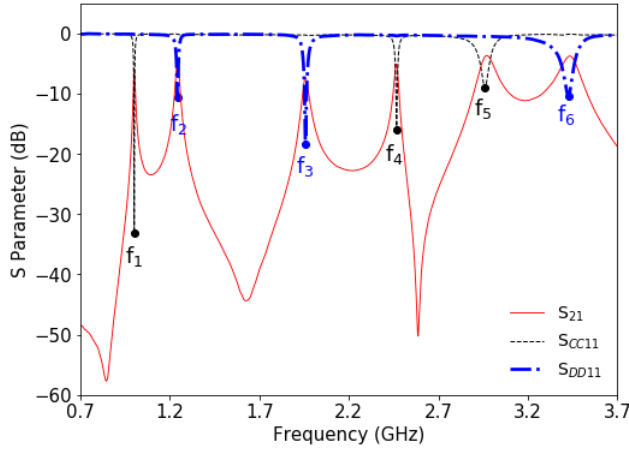


Fig. 5. Measured frequency response of the ECR sensor without liquid samples (i.e., empty). Differential-mode ( $S_{DD11}$ ) and common-mode ( $S_{CC11}$ ).

the differential-mode ( $S_{DD11}$ ) and common-mode ( $S_{CC11}$ ) are obtained using the following [31]:

$$S_{DD11} = 0.5 (S_{11} - S_{21} - S_{12} + S_{22}) \quad (5)$$

$$S_{CC11} = 0.5 (S_{11} + S_{21} + S_{12} + S_{22}) \quad (6)$$

where  $S_{11}$ ,  $S_{12}$ ,  $S_{21}$ , and  $S_{22}$  are the single-ended  $S$ -parameters. The transformation allows finding the precise resonant frequency, as shown in Fig. 5.

The corresponding dielectric constant relation for each liquid is

$$\begin{aligned} \epsilon'_{r_{n-KCL1}} &= \rho_{1n} f_{n-KCL1}^{\rho_{2n}} + \rho_{3n} \\ \epsilon'_{r_{n-KCL2}} &= \rho_{1n} f_{n-KCL2}^{\rho_{2n}} + \rho_{3n} \\ \epsilon'_{r_{n-KCL3}} &= \rho_{1n} f_{n-KCL3}^{\rho_{2n}} + \rho_{3n} \end{aligned} \quad (7)$$

where  $\epsilon'_{r_{n-KCL1}}$ ,  $\epsilon'_{r_{n-KCL2}}$ , and  $\epsilon'_{r_{n-KCL3}}$  are the KCL dielectric constants, and  $f_{n-KCL1}$ ,  $f_{n-KCL2}$ , and  $f_{n-KCL3}$  are the KCL obtained resonance frequencies;  $n$  represents the resonance frequency number, from 1 to 6.

#### IV. EXPERIMENTAL RESULTS

Measurements to determine the liquid's permittivity were performed using the proposed six-band ECR and methodology. During the experiments, the laboratory environment was maintained at stable 23 °C with a heat exchanger system. The measurements were made in a short period of time, avoiding temperature fluctuations. Several liquids were used in experiments, as follows: 1) DI water ( $H_2O$ ); 2) acetonitrile ( $C_2D_3N$ ); 3) methyl hydrate ( $CH_3OH$ ); 4) acetone ( $C_3H_6O$ ); 5) Isopropyl alcohol ( $C_3H_8O$ ); 6) chloroform ( $CHCl_3$ ); 7) castor oil ( $C_{57}H_{104}O_9$ ); 8) mineral oil (liquid paraffin); 9) toluene ( $C_7H_8$ ); 10) benzene ( $C_6H_6$ ); and 11) air. The volume of the liquid (120  $\mu$ L) was obtained using a micropipette (with a systematic error of  $\pm 0.6\%$ ) to ensure repeatability in the liquid measurements, and a segment of adhesive-backed copper foil was used to restore the GND plane. Each measurement was repeated five times using the same measuring instruments (the Anritsu MS4644B vector network analyzer calibrated with the

TABLE II  
EXPERIMENTAL RESONANCE FREQUENCIES

Liquid	$f_1$ (GHz)	$f_2$ (GHz)	$f_3$ (GHz)	$f_4$ (GHz)	$f_5$ (GHz)	$f_6$ (GHz)
1	0.867	1.036	1.747	2.149	2.788	2.683
2	0.894	1.075	1.795	2.202	2.825	2.886
3	0.898	1.088	1.812	2.228	2.845	3.025
4	0.918	1.123	1.834	2.248	2.854	3.038
5	0.955	1.189	1.909	2.366	2.928	3.322
6	0.972	1.206	1.917	2.381	2.926	3.309
7	0.986	1.224	1.935	2.431	2.941	3.368
8	0.992	1.231	1.944	2.442	2.952	3.383
9	0.990	1.228	1.941	2.428	2.947	3.374
10	0.990	1.228	1.941	2.435	2.947	3.379
11	1.001	1.244	1.957	2.467	2.970	3.436

TABLE III  
DIELECTRIC CONSTANT OF THE KNOWN CALIBRATION LIQUIDS

KCL	$\epsilon'_{r*}$					
	$f_1$	$f_2$	$f_3$	$f_4$	$f_5$	$f_6$
1	78.80	78.70	78.13	77.71	77.01	76.38
4	21.65	21.66	21.57	20.12	20.07	20.01
8	2.36	2.37	2.36	2.31	2.36	2.35

$\epsilon'_{r*}$  was obtained from the Keysight N1501A dielectric probe kit in [25].

TABLE IV  
FITTING CONSTANT VALUES

	$\rho_1$	$\rho_2$	$\rho_3$
$f_1$	3.80	-21.42	-2.016
$f_2$	138.2	-14.26	-4.760
$f_3$	$5.57 \cdot 10^7$	-24.06	-3.917
$f_4$	$1.18 \cdot 10^{12}$	-30.66	0.781
$f_5$	$6.3 \cdot 10^{27}$	-58.18	-0.167
$f_6$	$4.43 \cdot 10^5$	-8.67	-9.12

SOLT technique using the 3652A-K calibration kit), under the same room environmental conditions, and with only one operator doing the measurements. This process was implemented in order to reduce the errors deriving from the liquid volume, the temperature (room temperate), the measuring instruments, and the ground plane restoration. The measurements revealed a frequency shifting of around  $\pm 6.19$  MHz. Considering the resonant frequencies span as follows: 243 MHz between  $f_1$  and  $f_2$ , 713 MHz between  $f_2$  and  $f_3$ , 510 MHz between  $f_3$  and  $f_4$ , 503 MHz between  $f_4$  and  $f_5$ , and 466 MHz between  $f_5$  and  $f_6$ , then the frequency shifting error is lower, around 1.27%. Therefore, the average of the measurements was used. An example of the averaged measurements at the first and second resonance frequencies,  $f_1$  and  $f_2$ , for each liquid is shown in Fig. 6(a) and (b), respectively.

TABLE V  
RESULTS OF THE DIELECTRIC CONSTANT VALUES

Liq.	$f_1$			$f_2$			$f_3$			$f_4$			$f_5$			$f_6$		
	$\epsilon'_{r*}$	$\epsilon'_{r_{exp}}$	$\Delta E$	$\epsilon'_{r*}$	$\epsilon'_{r_{exp}}$	$\Delta E$	$\epsilon'_{r*}$	$\epsilon'_{r_{exp}}$	$\Delta E$	$\epsilon'_{r*}$	$\epsilon'_{r_{exp}}$	$\Delta E$	$\epsilon'_{r*}$	$\epsilon'_{r_{exp}}$	$\Delta E$	$\epsilon'_{r*}$	$\epsilon'_{r_{exp}}$	$\Delta E$
1	78.80	78.80	99.98%	78.70	78.70	99.98%	78.13	78.13	99.98%	77.71	77.71	99.98%	77.01	77.01	99.98%	76.38	76.38	99.98%
2		39.88			44.51			38.83		35.28 <sup>1</sup>	37.23	94.50%		34.30			36.30	
3	30.84	36.05	83.08%	29.86	31.66	93.97%	25.30	30.16	80.81%	22.84	26.21	85.20%	20.03	22.32	82.74%	18.14	21.11	83.62%
4	21.65	21.65	99.98%	21.66	21.66	99.98%	21.57	21.57	99.98%	20.12	20.12	99.98%	20.07	20.07	97.87%	20.01	20.01	99.98%
5	8.35	8.17	97.85%	7.43	6.94	93.38%	5.52	5.80	94.80%	5.00	4.81	96.20%	4.76	4.30	90.44%	4.53	4.31	95.06%
6		4.96			4.79			4.87			4.10			4.48			4.77	
7	3.16	3.12	98.84%	3.14	2.98	94.72%	3.06	3.10	98.65%	3.03	2.54	83.70%	2.99	3.28	90.31%	2.97	2.80	94.22%
8	2.36	2.36	99.98%	2.37	2.37	99.98%	2.36	2.36	99.98%	2.31	2.41	95.90%	2.36	2.36	99.98%	2.35	2.32	98.60%
9	2.69 <sup>2</sup>	2.69	99.94%	2.69 <sup>2</sup>	2.62	97.40%	2.68 <sup>2</sup>	2.60	96.89%	2.67 <sup>2</sup>	2.61	97.50%	2.66 <sup>2</sup>	2.89	90.98%	2.65 <sup>2</sup>	2.62	98.87%
10		2.69			2.62			2.60			2.45			2.89			2.47	

$\epsilon'_{r*}$  values were obtained from the Keysight N1501A dielectric probe kit in [25].  
<sup>1</sup>  $\epsilon'_{r*}$  reported in [7].  
<sup>2</sup>  $\epsilon'_{r*}$  reported in [32].

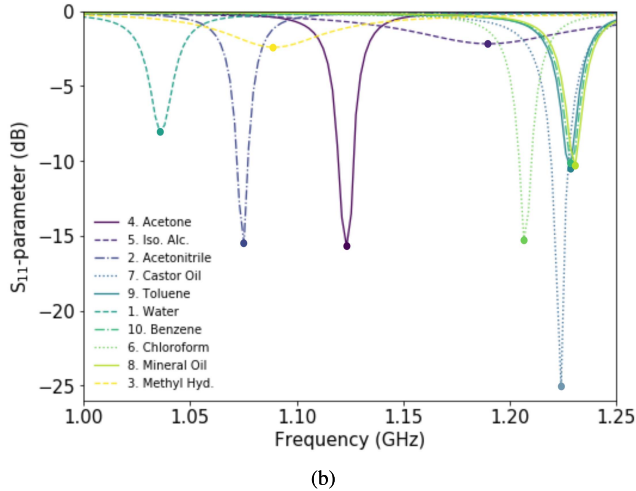
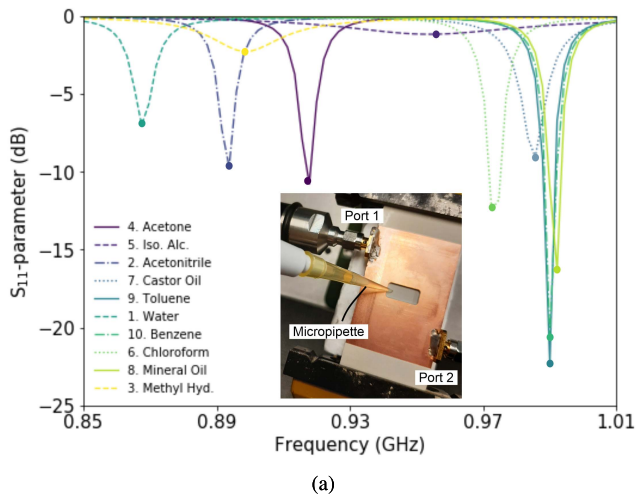


Fig. 6. Experimental frequency responses of liquids at (a)  $f_1$  and (b)  $f_2$ .

A photo of the six-band ECR sensor bottom view and the micropipette is inserted in Fig. 6(a). In addition, Table II summarizes the experimental resonance frequencies of the

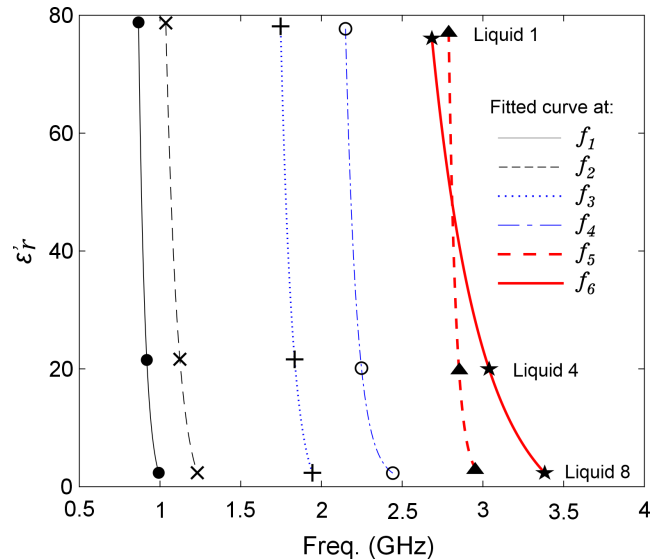


Fig. 7. Fit curves using the known calibration liquids, DI water (liquid 1), acetone (liquid 4), and mineral oil (liquid 8) at each resonance frequency.

KCLs at six resonance frequencies,  $f_{n-KCL}$ , where  $n$  represents each resonant frequency. DI water, acetone, and mineral oil (liquids 1, 4, and 8) were used as known calibration liquids (KCL1, KCL2, and KCL3) to determine the fitting constants  $\rho_{1n}$ ,  $\rho_{2n}$ , and  $\rho_{3n}$ . The dielectric constants ( $\epsilon'_{r*}$ ) of the KCLs were obtained from the Keysight N1501A dielectric probe kit and they are reported in [25] and those values are shown in Table III. The equation system in (7) is solved using MATLAB's Curve Fitting Toolbox at each resonant frequency and the results are summarized in Table IV. In addition, the curves fit and the KCLs at each resonance frequency are shown in Fig. 7.

In order to validate the fitting constants ( $\rho_{1n}$ ,  $\rho_{2n}$ , and  $\rho_{3n}$ ), the experimental resonance frequencies of the liquids 2, 3, 5–7, 9, and 10 in Table II, were used in (4) to obtain the experimental dielectric constants ( $\epsilon'_{r_{exp}}$ ), these results are

TABLE VI  
COMPARISON BETWEEN THE SIX-BAND ECR SENSOR AND OTHER WORKS

Characteristic	[21]	[30]	[33]	This work
Sensor topology	NID-SRRs	TL loaded with a shunt-connected series LC resonator	Meander Open CSRR	ECR
Resonant frequency (GHz)	5.76, 7.85	1.91	0.33	1.001, 1.244, 1.957, 2.467, 2.970, 3.436
Operation frequency range (empty-water)	5.76-4.80 7.85-6.35	1.91-1.30	0.33-0.204	1.001-0.867, 1.244-1.036, 1.957-1.747 2.467-2.149, 2.970-2.788, 3.436-2.683
Container material	NO	Polydimethylsiloxane	FR4	NO
Tested liquids	DI Water, Glucose, Methanol, Ethanol	DI Water, Methanol, Ethanol	DI Water, Ethanol	DI Water, Acetonitrile, Methyl hydrate, Acetone, Isopropyl alcohol, Chloroform, Castor oil, Mineral oil, Toluene, Benzene
Sensitivity	0.28, 0.30	0.415	0.504	0.17, 0.22, 0.14, 0.17, 0.08, 0.30

presented in Table V. The close agreement between the dielectric constants measured with the coaxial probe or reported in other works ( $\epsilon'_{r*}$ ) and the dielectric constants obtained in this work ( $\epsilon'_{r_{exp}}$ ), by mean of the relative error ( $\% \epsilon'_r$ ), is given by

$$\begin{aligned} \Delta E &= 100 - \% \epsilon'_r \\ &= 100 - \left( \frac{|\epsilon'_{r*} - \epsilon'_{r_{exp}}|}{\epsilon'_{r*}} \times 100 \right). \end{aligned} \quad (8)$$

In Table V, it can be observed that the close agreement at the first resonance frequency ( $f_1$ ) is over 97.85% except for liquid 3. At the second resonance frequency ( $f_2$ ),  $\% \epsilon'_r$  is more than 93.38% for all liquids. Similarly at  $f_1$ , other liquids show the  $\Delta E$  over 94.80%, 94.50%, 90.31%, and 94.22% at  $f_3$ ,  $f_4$ ,  $f_5$ , and  $f_6$ , respectively, except for liquid 3, where the  $\Delta E$  values are between 80.81% and 93.97%. In addition, liquid 7 shows a value over 80% at  $f_4$ . In terms of average, the result is higher than 94%, including the last two mentioned liquids. Thus, these results show highly competitive multifrequency sensor.

The relative sensitivity ( $S$ ) of the six-band ECR sensor is given by [21], [30], [33]

$$S = \frac{|f_{empty} - f_{SCL}|}{f_{empty} \cdot \Delta \epsilon'_r} \times 100 (\%) \quad (9)$$

where  $f_{empty}$  is the empty sensor resonance frequency,  $f_{SCL}$  is the standard comparison liquid (SCL) resonance frequency, and  $\Delta \epsilon'_r = \epsilon'_{r(SCL)} - 1$  is the dielectric constant variation. Table VI presents a comparison between this work and others previously presented, considering different characteristics, also shows the relative sensitivity of the six-band ECR sensor using DI water as the SCL. It is noticed that the proposed sensor is able to work at six resonant frequencies simultaneously, and it has been validated with several liquids.

## V. CONCLUSION

A new six-band microstrip ECR sensor for liquid characterization has been presented. The sensor has been designed to have a pocket milled through the dielectric of the substrate

to contain the liquid sample. The single-ended  $S$ -parameter transformation to differential and common modes was used to find the precise resonant frequencies. These frequencies were related to the real part of the permittivity, or dielectric constant, using the curve fitting method. A sensing methodology was implemented in a wide range of liquid's dielectric constant (from 2 to 79). The experimental results show close similarities to the dielectric constants reported in other works, and the sensitivity of the sensor is between 0.08 and 0.30.

## ACKNOWLEDGMENT

The authors would like to thank Ian Goode and Hayden Banting at Queen's University, Kingston, ON, Canada, for useful discussions and assistance with the sensor's fabrication.

## REFERENCES

- [1] L.-F. Chen, C. Ong, C. Neo, V. Varadan, and V. K. Varadan, *Microwave Electronics: Measurement and Materials Characterization*. Hoboken, NJ, USA: Wiley, 2004.
- [2] K. Saeed, M. F. Shafique, M. B. Byrne, and I. C. Hunter, "Planar microwave sensors for complex permittivity characterization of materials and their applications," in *Applied Measurement Systems*, Z. Haq, Ed. Rijeka, Croatia: InTech, Feb. 2012, pp. 319–350.
- [3] P. Vélez, L. Su, K. Grenier, J. Mata-Contreras, D. Dubuc, and F. Martín, "Microwave microfluidic sensor based on a microstrip splitter/combiner configuration and split ring resonators (SRRs) for dielectric characterization of liquids," *IEEE Sensors J.*, vol. 17, no. 20, pp. 6589–6598, Oct. 2017.
- [4] A. Javed, A. Arif, M. Zubair, M. Q. Mehmood, and K. Riaz, "A low-cost multiple complementary split-ring resonator based microwave sensor for contactless dielectric characterization of liquids," *IEEE Sensors J.*, vol. 20, no. 19, pp. 11326–11334, Oct. 2020.
- [5] S. Kiani, P. Rezaei, M. Navaei, and M. S. Abrishamian, "Microwave sensor for detection of solid material permittivity in single/multilayer samples with high quality factor," *IEEE Sensor J.*, vol. 18, no. 24, pp. 9971–9977, Dec. 2018.
- [6] Y. Khanna and Y. K. Awasthi, "Dual-band microwave sensor for investigation of liquid impurity concentration using a metamaterial complementary split-ring resonator," *J. Electron. Mater.*, vol. 49, no. 1, pp. 385–394, Jan. 2020.
- [7] G. Acevedo-Osorio, E. Reyes-Vera, and H. Lobato-Morales, "Dual-band microstrip resonant sensor for dielectric measurement of liquid materials," *IEEE Sensors J.*, vol. 20, no. 22, pp. 13371–13378, Nov. 2020.
- [8] L. Su, J. Mata-Contreras, P. Vélez, A. Fernández-Prieto, and F. Martín, "Analytical method to estimate the complex permittivity of oil samples," *Sensors*, vol. 18, no. 4, p. 984, 2018.

- [9] O. Korostynska, R. Blakey, A. Mason, and A. Al-Shamma, "Novel method for vegetable oil type verification based on real-time microwave sensing," *Sens. Actuators A, Phys.*, vol. 202, pp. 211–216, Nov. 2013.
- [10] F. S. Jafari and J. Ahmadi-Shokouh, "Reconfigurable microwave SIW sensor based on PBG structure for high accuracy permittivity characterization of industrial liquids," *Sens. Actuators A, Phys.*, vol. 283, pp. 386–395, Nov. 2018.
- [11] N. K. Tiwari, S. P. Singh, and M. J. Akhtar, "Novel improved sensitivity planar microwave probe for adulteration detection in edible oils," *IEEE Microw. Wireless Compon. Lett.*, vol. 29, no. 2, pp. 164–166, Feb. 2019.
- [12] A. Mirbeik-Sabzevari and N. Tavassolian, "Characterization and validation of the slim-form open-ended coaxial probe for the dielectric characterization of biological tissues at millimeter-wave frequencies," *IEEE Microw. Wireless Compon. Lett.*, vol. 28, no. 1, pp. 85–87, Jan. 2018.
- [13] S. Saha *et al.*, "A glucose sensing system based on transmission measurements at millimetre waves using micro strip patch antennas," *Sci. Rep.*, vol. 7, no. 1, pp. 1–11, Dec. 2017.
- [14] W. Liu, X. Yang, Y. Niu, and H. Sun, "Improve planar multiple split-ring sensor for microwave detection applications," *Sens. Actuators A, Phys.*, vol. 297, Oct. 2019, Art. no. 111542.
- [15] M. H. Zarifi, M. Rahimi, M. Daneshmand, and T. Thundat, "Microwave ring resonator-based non-contact interface sensor for oil sands applications," *Sens. Actuators B, Chem.*, vol. 224, pp. 632–639, Mar. 2016.
- [16] K. Saeed, A. C. Guyette, I. C. Hunter, and R. D. Pollard, "Microstrip resonator technique for measuring dielectric permittivity of liquid solvents and for solution sensing," in *IEEE MTT-S Int. Microw. Symp. Dig.*, Jun. 2007, pp. 1185–1188.
- [17] C. G. Juan, E. Bronchalo, B. Potelon, C. Quendo, E. Avila-Navarro, and J. M. Sabater-Navarro, "Concentration measurement of microliter-volume water–glucose solutions using  $Q$  factor of microwave sensors," *IEEE Trans. Instrum. Meas.*, vol. 68, no. 7, pp. 2621–2634, Jul. 2019.
- [18] N. Sharafadinzadeh, M. Abdolrazzagh, and M. Daneshmand, "Investigation on planar microwave sensors with enhanced sensitivity from microfluidic integration," *Sens. Actuators A, Phys.*, vol. 301, Jan. 2020, Art. no. 111752.
- [19] J. Wu *et al.*, "Design and validation of liquid permittivity sensor based on RCRR microstrip metamaterial," *Sens. Actuators A, Phys.*, vol. 280, pp. 222–227, Sep. 2018.
- [20] A. A. Abduljabar, H. Hamzah, and A. Porch, "Multi-resonators, microwave microfluidic sensor for liquid characterization," *Microw. Opt. Technol. Lett.*, vol. 63, no. 4, pp. 1042–1047, Apr. 2021.
- [21] S. Kiani, P. Rezaei, and M. Navaei, "Dual-sensing and dual-frequency microwave SRR sensor for liquid samples permittivity detection," *Measurement*, vol. 160, Aug. 2020, Art. no. 107805.
- [22] J.-S. Hong and M. J. Lancaster, "Couplings of microstrip square open-loop resonators for cross-coupled planar microwave filters," *IEEE Trans. Microw. Theory Techn.*, vol. 44, no. 11, pp. 2099–2109, Nov. 1996.
- [23] M. H. Zarifi and M. Daneshmand, "Wide dynamic range microwave planar coupled ring resonator for sensing applications," *Appl. Phys. Lett.*, vol. 108, no. 23, Jun. 2016, Art. no. 232906.
- [24] L. V. Herrera-Sepulveda, J. L. Olvera-Cervantes, A. Corona-Chavez, and T. Kaur, "Sensor and methodology for determining dielectric constant using electrically coupled resonators," *IEEE Microw. Wireless Compon. Lett.*, vol. 29, pp. 626–628, Sep. 2019.
- [25] H. Banting and C. E. Saavedra, "Dielectric spectroscopy of fluids and polymers for microwave microfluidic circuits and antennas," *IEEE Trans. Microw. Theory Techn.*, vol. 69, no. 1, pp. 337–343, Jan. 2021.
- [26] L.-V. Herrera-Sepulveda, J.-L. Olvera-Cervantes, A. Corona-Chavez, and T. Kaur, "New methodology to determine the loss tangent of dielectric planar samples by using electrically coupled resonators," *J. Electromagn. Waves Appl.*, vol. 34, no. 18, pp. 2410–2418, Dec. 2020.
- [27] H. F. Laminates, *Ro Series Circuit Materials*. Chandler, AZ, USA: Rogers Corp., 2018. [Online]. Available: <https://www.rogerscorp.com>
- [28] J.-S. G. Hong and M. J. Lancaster, *Microstrip Filters for RF/Microwave Applications*, vol. 167. Hoboken, NJ, USA: Wiley, 2004.
- [29] R. Garg, I. Bahl, and M. Bozzi, *Microstrip Lines and Slotlines*. Norwood, MA, USA: Artech House, 2013.
- [30] A. Ebrahimi, J. Scott, and K. Ghorbani, "Ultrahigh-sensitivity microwave sensor for microfluidic complex permittivity measurement," *IEEE Trans. Microw. Theory Techn.*, vol. 67, no. 10, pp. 4269–4277, Oct. 2019.
- [31] A. Arbelaez-Nieto, E. Cruz-Perez, J.-L. Olvera-Cervantes, A. Corona-Chavez, and H. Lobato-Morales, "The perfect balance—A design procedure for balanced bandpass filters [application notes]," *IEEE Microw. Mag.*, vol. 16, no. 10, pp. 54–65, Nov. 2015.
- [32] J. Lou, T. Hatton, and P. Laibinis, "Effective dielectric properties of solvent mixtures at microwave frequencies," *J. Phys. Chem. A*, vol. 101, no. 29, pp. 5262–5268, 1997.
- [33] C.-S. Lee, B. Bai, Q.-R. Song, Z.-Q. Wang, and G.-F. Li, "Open complementary split-ring resonator sensor for dropping-based liquid dielectric characterization," *IEEE Sensors J.*, vol. 19, no. 24, pp. 11880–11890, Aug. 2019.

**Lyda Vanessa Herrera Sepulveda** received the B.Sc. degree from the Universidad Industrial de Santander, Santander, Colombia, in 2013, and the M.Sc. and Ph.D. degrees from the Instituto Nacional de Astrofísica, Óptica y Electrónica, Puebla, México, in 2017 and 2021, respectively, all in electronics engineering.

In 2020, she joined as a Ph.D. Visiting Researcher with the Millimeter-Wave Electronics Group, Queen's University, Kingston, ON, Canada, where she became a Post-Doctoral Fellow in 2021. Her research interests include microwave planar structures characterization for sensing applications and new technologies for microwave sensors, with a focus on resonators.

**Jose Luis Olvera Cervantes** received the B.Sc. degree from the Instituto Politécnico Nacional, Mexico City, Mexico, in 2001, and the M.Sc. and Ph.D. degrees from the Centro de Investigación Científica y de Educación Superior de Ensenada, Ensenada, Mexico, in 2005 and 2008, respectively.

In 2009, he joined the Instituto Nacional de Astrofísica, Óptica y Electrónica, where he is currently a Full Professor. His research interests include microwave sensors, radar systems, dielectric characterization, food properties, and signal processing.

**Carlos E. Saavedra** is currently a Professor and the Head of the Department of Electrical and Computer Engineering at Queen's University, Kingston, ON, Canada. He holds the B.Sc. degree from the University of Virginia, Charlottesville, VA, USA, and the M.Sc. and Ph.D. degrees from Cornell University, Ithaca, NY, USA, all in electrical engineering. He is a licensed Professional Engineer (P.Eng.) in the Province of Ontario. During Sabbatical leaves, he has held visiting appointments at the University of Navarra, Pamplona, Spain, the Universidade Federal of Rio Grande do Sul, Rio Grande, Brazil, and the University of Twente, Enschede, Holland. From 1998 to 2000, he was a Senior Engineer at Millitech Corporation, Northampton, MA, USA.

Prof. Saavedra is the former Co-Chair of the Natural Sciences and Engineering Research Council of Canada (NSERC) Discovery Grant Evaluation Group for Electrical and Computer Engineering and he has served on grant review panels at the National Science Foundation (USA) and as an External Reviewer for the Netherlands Organization for Scientific Research. He is a Guest Editor of the IEEE OPEN JOURNAL OF ANTENNAS AND PROPAGATION and has previously served as an Associate Editor of the IEEE TRANSACTIONS ON MICROWAVE THEORY AND TECHNIQUES and as Guest Editor of the *IEEE Microwave Magazine*.